

Permeability Measurements of Thin Film Using a Flexible Microstrip Line-Type Probe Up To 40 GHz

S. Yabukami, K. Kusunoki*, H. Uetake, H. Yamada*, T. Ozawa, R. Utsumi**, T. Moriizumi***, and Y. Shimada****

Tohoku Gakuin University, 1-13-1 Chuo, Tagajo 985-8537, Japan

*Sendai National College of Technology, 48 Nodayama, Medeshima-Shiote, Natori 981-1239, Japan

**Toei Scientific Industrial Company Ltd., 1-101-60 Medeshimadai, Natori 981-1251, Japan

***Cadox Systems Inc., 15-21 Oshiage-Cho, Gyoda 361-0045, Japan

****Graduate School of Engineering, Tohoku University, 6-6-05 Aramaki Aza Aoba, Aoba-ku, Sendai 980-8579, Japan

A highly sensitive probe based on the skin effect was developed to measure thin film permeability. A new microstrip-line-type probe on a flexible substrate was fabricated and placed in contact with a magnetic thin film. The probe enhanced the signal-to-noise ratio and broadband measurement. The permeability of amorphous CoNbZr film (25 mm × 25 mm, 5 nm thick) and that of CoFeB film (45 mm × 25 mm, 0.5 μm thick) were optimized. The measured values were in rough agreement with theoretical values based on the Landau–Lifshitz–Gilbert equation and eddy current generation up to 40 GHz.

Key words: flexible microstrip-line-type probe, skin effect, permeability, very thin film

1. Introduction

High frequency permeability of very thin magnetic films is important because sensing devices and spintronic devices are fabricated from such film (film thickness of less than 10 nm). However, almost all permeameters^{1)–3)} require a special sample, usually no more than several millimeters in width and more than 100 nm in thickness. Exceedingly few permeameters can measure thin film over 30 GHz continuously.

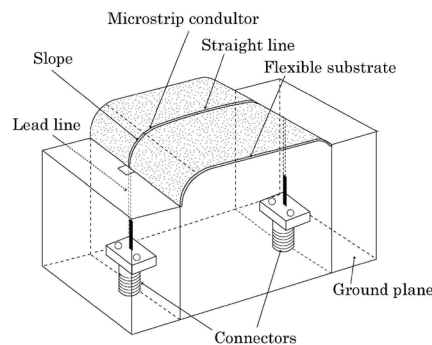
As previously reported, we have developed a microstrip-line-type probe⁴⁾. The probe is not always applicable for evaluation of very thin film, such as that less than 10 nm in thickness, because of the low signal-to-noise ratio. Subsequently, we also developed a straight microstrip-line-type probe on a flexible polyimide substrate⁵⁾. However, the probe resonates at a frequency of over 7 GHz because of impedance mismatch and is not applicable for large samples.

In the present study, we developed a new probe composed of a straight microstrip line on a flexible substrate, the microstrip line sloping to meet the lead line at either end. The flexibility of the probe enables contact between it and a magnetic thin film, which enhances the signal-to-noise ratio. The probe, including the microstrip line and lead lines, has a characteristic impedance of around 50 ohm. As a result, the permeability of very thin film was evaluated up to 40 GHz.

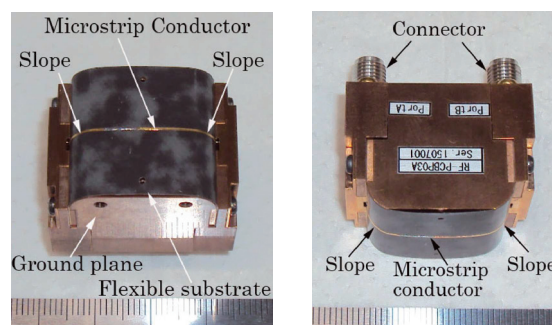
2. Experimental setup

2.1 A new probe and system setup

Fig. 1(a) shows a schematic diagram of the probe. Figs. 1(b) and (c) show a photograph of the probe. The new probe is composed of a straight microstrip conductor (15 mm in length, 0.36 mm in width) on a flexible substrate (RT/duroid® 5870, 130 μm in



(a) oblique drawing



(b) top view

(c) side view

Fig. 1 Schematic view of probe.

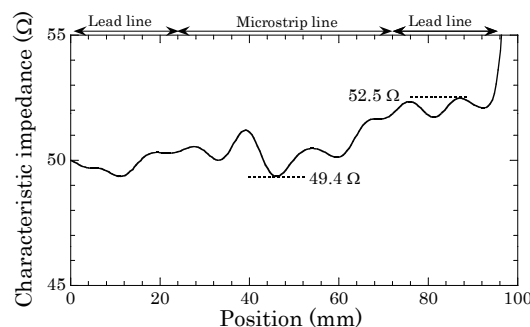


Fig. 2 Characteristic impedance of the probe obtained from time-domain reflectometry (TDR) measurements.

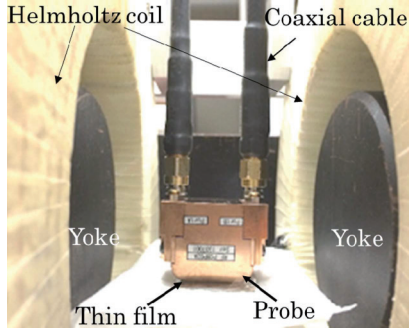


Fig. 3 Photograph of the probe and film.

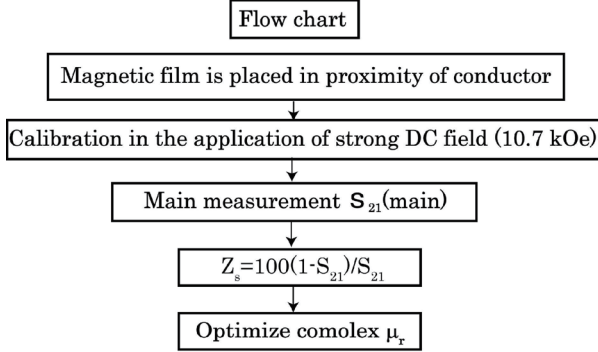


Fig. 4 Flow chart of the permeability measurements.

thickness, $\epsilon_r=2.3$), a ground plane, lead lines, and two connectors. The microstrip line has slopes to maintain a characteristic impedance of around 50Ω and to allow close contact of a large sample with the probe. A magnetic thin film coated with photo-resist (about $8 \mu\text{m}$ in thickness) is in contact with the microstrip conductor. Coaxial cables are connected to a network analyzer. The probe can be easily bent because of the flexibility of the substrate, enabling a good fit between the probe and the thin film, resulting in improved signal-to-noise ratio.

Fig. 2 shows the characteristic impedance of the probe measured by time domain reflectometry (Agilent Technologies N5227A). The characteristic impedance was 49.4Ω - 52.5Ω along the microstrip line.

The system setup was the same as the previous works^{4,5}. Fig. 3 shows a photograph of the probe, a magnetic film, a Helmholtz coil, and a micrometer. The spacing between the probe and the film is adjusted by a micrometer. An Fe yoke (80 mm in diameter) is arranged around the bias coil to increase the dc magnetic field.

2.2 Optimization of permeability

Fig. 4 shows a flow chart of permeability optimization. Firstly, S_{21} is calibrated by application of a strong dc field (around 850.65 kA/m (10.7 kOe)) in the direction of the easy axis to saturate the magnetic film. Secondly, S_{21} is measured without a strong dc field, and then the complex impedance is calculated by equation (1).

$$Z_s = 100 (1 - S_{21}) / S_{21} \quad (1)$$

The S_{21} and Z_s include the multiple reflections in equation (1). Complex permeability is optimized using the Newton–Raphson method⁶) to take the skin effect of the magnetic film into account by using equations (2) - (4),

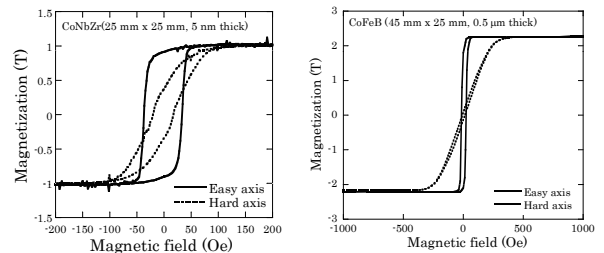
$$Z_s = \frac{k_s \rho l}{2w} \coth\left(\frac{k_s t}{2}\right) - \left\{ \frac{k'_s \rho l}{2w} \coth\left(\frac{k'_s t}{2}\right) \right\} \frac{1}{S_{21}} \quad (2)$$

$$k_s = \frac{(1+j)}{\sqrt{\frac{\rho}{\pi f \mu_r \mu_0}}} \quad (3) \quad k'_s = \frac{(1+j)}{\sqrt{\frac{\rho}{\pi f \mu_r^{ref} \mu_0}}} \quad (4)$$

where ρ is the resistivity of the film, t is the film thickness, l is the microstrip line length, w is the width of the microstrip conductor, and μ_r^{ref} is relative permeability when a strong dc field of 10.7 kOe was applied. The high frequency current induces a magnetic field in the width direction of the conductor pattern, and the magnetic field and the eddy current are localized in the skin of the magnetic film^{4,5}).

3. Experimental results

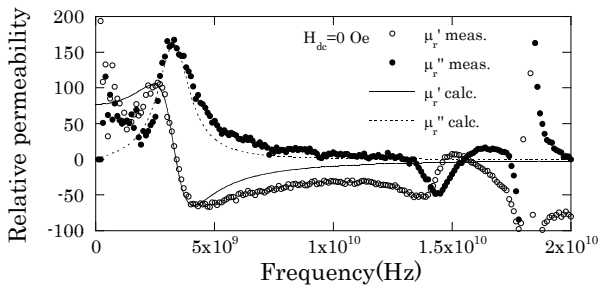
Fig. 5 shows the MH curves of $\text{Co}_{85}\text{Nb}_{12}\text{Zr}_3$ film and CoFeB film. Fig. 5(a) shows the MH curve of CoNbZr film ($25 \text{ mm} \times 25 \text{ mm}$ and 5 nm in thickness). The CoNbZr film was deposited by RF sputtering. The solid line shows the MH curve of the easy axis, and the dotted line shows that of the hard axis. The resistivity of the film was about $1.52 \times 10^{-6} \Omega\text{m}$ ($152 \mu\Omega\text{cm}$), which was slightly higher than that of bulky CoNbZr ($120 \mu\Omega\text{cm}$). An anisotropy field of around 70 Oe was observed. The anisotropy field was comparatively larger than that of previous studies^{7,8}), which is probably because the CoNbZr film was partly crystallized. However the perpendicular anisotropy that has often been observed for partially crystallized CoNbZr films is not seen for the sample probably because of intensified shape anisotropy of 5 nm thickness. Fig. 5(b) shows the MH curve of the CoFeB film ($45 \text{ mm} \times 25 \text{ mm}$ and $0.5 \mu\text{m}$ in thickness). The film was deposited by Carousel Sputtering⁹). Saturation magnetization around 2.2 T and an anisotropy field (H_k) of around 260 Oe was observed from the MH curve.



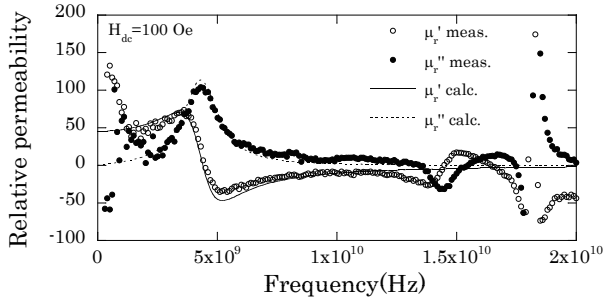
(a) CoNbZr film

(b) CoFeB film

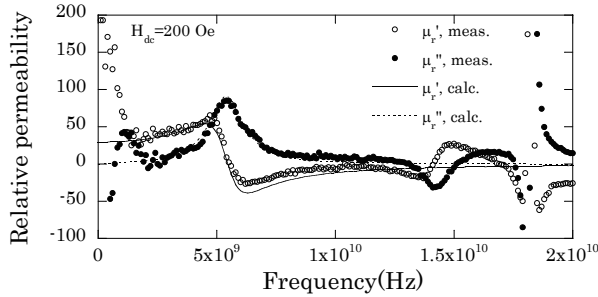
Fig. 5 MH curve of the film sample.



(a) No bias field



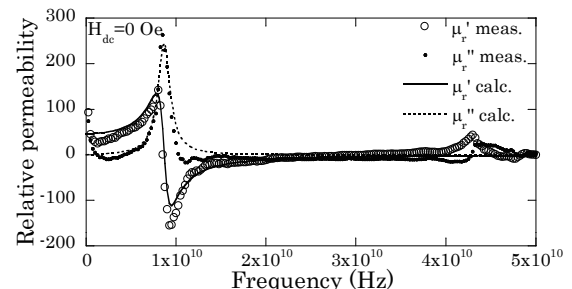
(b) $H_{dc}=100$ Oe



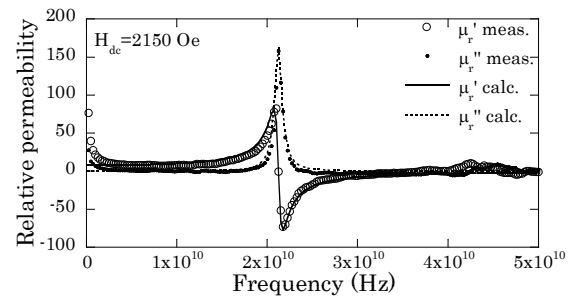
(c) $H_{dc}=200$ Oe

Fig. 6 Relative permeability of CoNbZr film (25 mm x 25 mm, 5 nm thick).

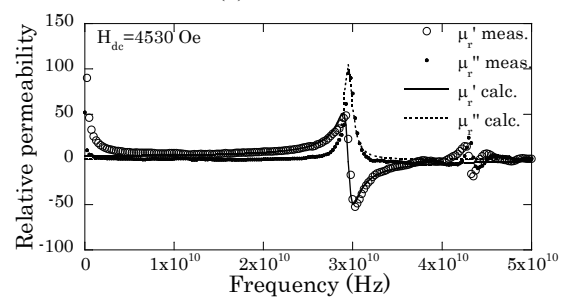
Fig. 6 shows the hard-axis permeability of amorphous CoNbZr film (25 mm x 25 mm, 5 nm in thickness) when it was in contact with the flexible probe. Fig. 6 (a) shows the permeability without the bias field, and (b) and (c) show the permeability when bias fields of 100 and 200 Oe, respectively, were applied along the easy axis. The symbols show measured permeability, and the dotted lines and the solid lines show the theoretical permeability based on the Landau–Lifshitz–Gilbert equation and eddy current generation¹⁰⁾, respectively. A g factor of 2.13¹¹⁾ was used to calculate theoretical permeability. An α (damping factor) of 0.04 was used to fit theoretical permeability to measured spectra. The absolute permeability was calibrated by the application of dc magnetic fields in the direction of the easy axis. The measured permeability roughly corresponded to the theoretical permeability up to 14 GHz. The ferromagnetic resonances were observed, and the resonance frequency was found to shift as the bias field increased. The signal to noise ratio in lower frequency decreased and the ferromagnetic resonance frequency was higher than that in the previous report⁵⁾, which was because the present system consist of magnetic core, therefore small leakage field of the yoke increased the resonance frequency even if the DC current was



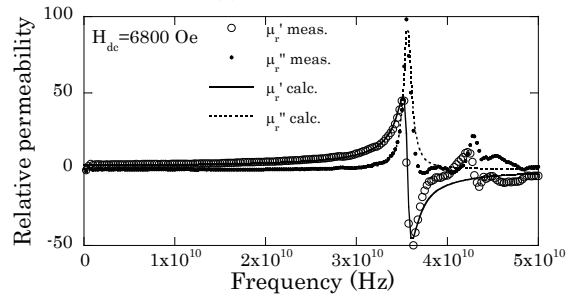
(a) No bias field



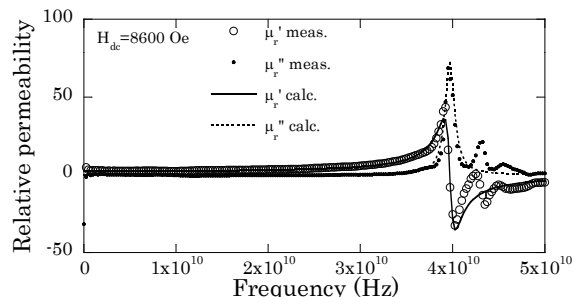
(b) $H_{dc}=2150$ Oe



(c) $H_{dc}=4530$ Oe



(d) $H_{dc}=6800$ Oe



(e) $H_{dc}=8600$ Oe

Fig. 7 Relative permeability of CoFeB film (45 mm x 25 mm, 0.5 μ m thick).

zero.

Fig. 7 shows the hard-axis permeability of CoFeB film (45 mm x 25 mm, 0.5 μ m in thickness). Fig. 7 (a) shows the permeability without a bias field, and

Figs. 7 (b)–(e) show the permeability when bias fields of 2150, 4530, 6800, and 8600 Oe were applied along the easy axis. Symbols show measured permeability, and the dotted lines and solid lines show the theoretical permeability based on the Landau–Lifshitz–Gilbert equation and eddy current generation¹⁰, respectively. An α (damping factor) of 0.02 and a g factor of 2.13 were used to calculate theoretical permeability. The absolute permeability was calibrated by the application of dc magnetic fields in the direction of the easy axis. The measured permeability was found to roughly correspond to theoretical permeability up to 40 GHz. Ferromagnetic resonance shifted from 8 to 40 GHz as the dc field increased. A sharp change was observed around 42–43 GHz. This limit originated from the ferromagnetic resonance of the magnetic film with a strong bias field of about 10.7 kOe.

4. Conclusions

1. A highly sensitive probe was developed to measure very thin film permeability using a straight microstrip line and a flexible substrate.
2. A CoNbZr film (25 mm x 25 mm, 5 nm in thickness) was evaluated and the measured permeability was in rough agreement with the theoretical permeability up to 14 GHz.
3. A CoFeB film (45 mm x 25 mm, 0.5 μm in thickness) with a high anisotropy field was evaluated, and measured permeability was in rough agreement with the theoretical permeability up to 40 GHz.

Acknowledgments We would like to thank Prof. Munakata at Sojo University for providing the CoFeB film, Mr. Fujita of Japan Science and Technology Bureau for his advice, Dr. Nakai of Industrial

Technology Institute, Miyagi Prefectural Government for his help in measurement of MH-curves, and the Machine Shop of Tohoku Gakuin University for help in fabricating the probe. This work was supported in part by the Program for Revitalization Promotion of JST.

References

- 1) P. A. Calcagno, D. A. Thompson: *Rev. Sci. Instrum.*, **46**, 904 (1975).
- 2) M. Yamaguchi, S. Yabukami and K.I. Arai: *IEEE Trans. Magn.*, **32**, 4941 (1996).
- 3) H. B. Weir: *Proc IEEE*, **62**, 33 (1975).
- 4) T. Kimura, S. Yabukami, T. Ozawa, Y. Miyazawa, H. Kenju, Y. Shimada: *J. Magn. Soc. Jpn.* **38**, pp. 87-91 (2014).
- 5) K. Kusunoki, S. Yabukami, T. Ozawa, H. Uetake, H. Yamada, Y. Miyazawa, Y. Shimada: *J. Magn. Soc. Jpn.* **39**, pp. 111-115 (2015).
- 6) W.H. Press, S.A. Teukolsky, W.T. Vetterling and B.P. Flannery: *Numerical Recipes in C (Japanese Edition)*, pp.251–281, (Gijutsu Hyoron sha, Tokyo, 1993).
- 7) H. Katada, T. Shimatsu, I. Watanabe, H. Muraoka, Y. Nakamura and Y. Sugita: *J. Magn. Soc. Jpn.*, **24**, 539 (2000).
- 8) M.L. Schneider, A.B. Kos, and T.J. Silva: *Applied Physics Letters*, **85**, 254 (2004).
- 9) M. Namikawa, M. Munakata, M. Yagi, M. Motoyama, Y. Shimada, S. Yabukami, M. Yamaguchi, and K.I. Arai: *J. Magn. Soc. Jpn.*, **27**, 371 (2003).
- 10) Y. Shimada, J. Numazawa, Y. Yoneda and A. Hosono: *J. Magn. Soc. Jpn.*, **15**, 327(1991).
- 11) A. Yoshihara, K. Takanashi, M. Shimada, O. Kitakami and Y. Shimada: *Jpn. J. Appl. Phys.* **33**, 3927 (1994).

Received Feb. 10, 2016; Revised Aug. 26, 2016; Accepted Jan. 10, 2017